Simultaneous *operando* FTIR & Raman characterization (IRRaman) for the extended study of gas-phase reactions with solid catalysts

J. J. Ternero-Hidalgo[1], M.O. Guerrero-Pérez[1], J. Rodríguez-Mirasol[1], T. Cordero[1], M. A. Bañares[2*], R. Portela[2], P. Bazin[3], G. Clet[3], M. Daturi[3*]*

[1] Universidad de Málaga, Departamento de Ingeniería Química, E29071 Málaga, Spain

[2] Instituto de Catálisis y Petroleoquímica, CSIC, E28049 Madrid, Spain

[3] Normandie Univ, ENSICAEN, UNICAEN, CNRS, LCS, 14000 Caen, France

KEYWORDS: operando; IR; Raman; heterogeneous catalysis; VO_x/ZrO_2; propane ODH.

ABSTRACT

Simultaneous *operando* Raman and transmission FTIR spectroscopic measurements have been specifically coupled in a new homemade reactor setup designed in a joint CSIC-UNICAEN collaboration. FTIR and Raman spectroscopies allow respectively the simultaneous characterization of the adsorbed species or reaction intermediates, and yield structural information of the catalyst. This system was validated by applying to the study of vanadium based catalysts during propane OxyDeHydrogenation (ODH). The combined use of these spectroscopies with the activity results contributes to the understanding of propane ODH and the identification of the role of different oxygen species bound to vanadium sites. For example, the simultaneous characterization under the same conditions of the catalyst by IR and Raman confirms that the V=O mode has the same frequency in both spectroscopies, and that bridging oxygen sites (V-O-V, V-O-Zr) present higher activity than terminal V=O bonds. These results demonstrate the high potential of the new simultaneous transmission IR-Raman *operando* rig to correlate the activity and the structure of catalysts, thus assisting the rational design of catalytic processes.

Introduction

The relationships between the surface structure and the performance of the catalysts operating under relevant reaction conditions is an indispensable information to understand the catalytic mechanisms of reaction and deactivation and to identify the active phases for the rational design of more efficient catalytic materials. In this sense, there has been an increasing interest in the development of characterization techniques of functional materials under real operating conditions. Recent reviews [1–12] show the evolution of *in situ* and *operando* spectroscopic researches and their importance. *In situ* and *operando* techniques have been applied with different characterization techniques, such as IR [2-4, 13-17], EPR [18-19], synchrotron based techniques [5,20–21], Raman [6–8,22–30], NMR [9,10], UV-VIS [11] or TEM [1,12]. All those works show the high value of the information obtained from the simultaneous tracking of the catalysts structure and reactivity in order to design catalytic materials and processes in a rational way. There is still need for progress in the frame of time-resolved spectroscopy, design of high quality reaction-cells, development of techniques for the study of interfaces, and, particularly, multimodal *operando* approaches. Since each characterization technique can provide only a part of the picture, one of the main challenges to rise would be the development of tools that allow the possibility of combining different spectroscopic techniques in a single rig, when this can provide complementary insights into catalyst behavior.

Few works report the use of different characterization techniques for the simultaneous study of structural changes of the catalytic material and the

reaction medium. Among these multimodal *operando* approaches, Baiker *et al.*[31] performed a combined liquid-phase ATR-IR and XAS study during the aerobic oxidation of benzyl alcohol over Pd based catalysts. They combined both spectroscopic techniques for characterizing the catalytic materials and monitored the catalytic activity using FTIR spectroscopy, obtaining information about the particle structure/oxidation state (by XAS) and the surface species (by ATR-IR). Weckhuysen's group [32] designed a laboratory setup for combined *operando* X-ray diffraction and Raman spectroscopy of catalysts, with analysis of reaction products by gas chromatography. They used such setup for the study of the long-term deactivation of Co based catalysts during Fischer-Tropsch synthesis. The same group also combined XAFS, Raman and UV-Vis spectroscopies in a single experiment [33]. The combination of XAS, XRD and Raman for phase speciation in Water Gas Shift reaction catalysts has also been performed [34]. The *operando* coupling of EPR, Raman and UV-Vis spectroscopies was reported by Bruckner [35]. Other similar examples are highlighted in a review by Bentrup [36]. These examples demonstrate how the coupling of complementary *operando* techniques in one rig results in more rational and comprehensive information, necessary for the efficient design of catalytic materials.

The combination of Raman and IR spectroscopies is particularly convenient for supported oxides [37], since Raman spectroscopy reports essentially the structure of the supported phase while IR has more sensitivity to adsorbed species. Payen *et al.* [38] performed alternate *in situ* characterization by Raman and IR of Pd based catalysts for $DeNO_x$ using a commercial Raman spectrometer with an IR extension (Horiba Jobin Yvon). Zhang *et al.* [39-40] designed a home-made

high throughput reactor that combines FTIR and Raman spectroscopies. That setup has six parallel reaction channels with six Raman probes that allow studying the catalysts, while FTIR imaging allows the gas product analysis. Urakawa [41] designed a DRIFTS-Raman setup configuration that enables simultaneous IR-Raman detection with high spatial resolution in order to monitor the surface of catalysts under NO_x storage reduction. These contributions underline the complementarily of both measurements. It should be noted, however, that two main drawbacks are encountered: the measurements are not always simultaneous, and, in many cases, IR data rely on the use of DRIFTS or ATR-IR, two precious techniques which are however not directly quantitative and usually have a lower sensitivity since the scattered signal can be weak, and thus more difficult to interpret. Quantitative data are nevertheless required to elucidate the catalyst role for many reactions and to properly perform spectrokinetic studies [42]. The approach developed here will thus rather use transmission IR spectroscopy coupled to Raman to overcome this problem. Transmission FT-IR will directly provide quantitative signals for adsorbed molecular species, while Raman will inform on the structural aspects of the material at work, focusing on neighboring sample spots of a single sample, in exactly the same reaction conditions and with full temporal consistency.

Thus, the present paper reports the design and use of a novel concept of *operando* IR-Raman cell (the “IRRaman” *operando* reactor), in order to obtain, in a single experiment, with space and time consistency, transmission FTIR and Raman spectra of catalysts, coupled with online analysis of the reaction products under real operating conditions. Therefore, information about the structure of the catalyst (mainly from Raman), information of adsorbed species

(mainly from FTIR) and reactivity (online activity measurements) blend into a single experiment. The usefulness of this multimodal *operando* rig is demonstrated here though the study of the propane ODH reaction over V-Zr-O catalysts. Propane ODH has been largely studied [43-47]. Dispersed vanadia or molybdena-based catalysts are well known as active catalytic materials for this process.[45] The reaction mechanism shows that surface monomeric and polymeric species are active and participate in the formation of propyl or (iso)propoxy species as first reaction intermediates, which are usually further oxidized giving rise to CO_x in the gas phase [43]. The evolution of the solid catalyst during the pre-activation treatment and afterwards under the reaction flow will thus be followed here with the IRRaman *operando* reactor we have developed and compared with the development of the adsorbed species.

Experimental section

Catalysts synthesis. The synthesis of the catalytic materials has been previously described [48]. Briefly, Zirconium (IV) propoxide solution (Sigma-Aldrich, CAS: 23519-77-9, 70 wt. % in 1-propanol), polyvinylpyrrolidone (PVP) (Sigma-Aldrich, CAS: 9003-39-8, Mw ~1,300,000), acetylacetone (Sigma-Aldrich, CAS: 123-54-6, ≥99%), 1-propanol (Sigma-Aldrich, CAS: 71-23-8, ≥99.5%) and vanadyl acetylacetonate (Sigma-Aldrich, CAS: 3153-26-2, ≥97.0%) were used as starting materials. The polymer solutions for the electrospinning process were prepared by dissolving the zirconium precursor and PVP in 1-propanol solvent: 2.100 g of (zirconium (IV) propoxide), 0.317 g of PVP, 0.450 g of acetylacetone and 2.984 g of 1-propanol. Then, the vanadyl

acetylacetonate was added to the above polymer solution, to obtain final fibers with nominal vanadium mass concentrations of 2.5% (Zr-V2.5), 5.0% (Zr-V5.0) and 6.4% (Zr-V6.4). Subsequently, the polymer solutions were vigorously stirred for 24 h at room temperature before the electrospinning process. The electrospinning equipment has been already described in the previous articles [48-49]. Then, the electrospun fibers were calcined in a conventional tubular furnace. In each case, the heating rate was 10 ºC·min^{-1} up to 500 ºC, which was kept for 6 h in air flow (150 mL·min^{-1} STP) in order to eliminate the organic part and the remaining solvent and stabilize the zirconia fibers. The vanadium mass concentrations obtained by XPS analysis of these final samples Zr-V2.5, Zr-V5.0 and Zr-V6.4 were 2.7, 4.9 and 6.0%, respectively, as reported in a previous work [48-49].

The "IRRaman" reactor. The IR-Raman *operando* rig was specifically designed at Laboratoire Catalyse et Spectrochimie (Caen, France), adapting a home-made *operando* IR reactor-cell [50] to also host a Raman probe (Figure 1). This cell is a genuine catalytic reactor, both from the point of view of the fluidodynamics of the cavity [51] and in the preservation of the morphology of the self-supported wafer [52]. Evolutions of the so-called "Sandwich" *operando* IR cell have already been carried out in the past in order to facilitate the kinetic analysis [51] or to determine the reaction mechanisms in photocatalysis [53]. The adaptations made in the framework of this study aim to collect continuously both the transmission FTIR and reflectance Raman spectra on the same pellet (~20-30 mg, 2 cm²). Therefore, the cell was modified by notably replacing the two KBr windows positioned on one side of the cell by a stainless steel cylinder

drilled to accommodate the Raman probe with the lens placed a few millimeters close to the pellet and at the same time to let the IR beam pass through a dedicated small KBr window. The sealing of the cell was guaranteed via Kalrez O-rings. The diameter of the cylinder through which the IR beam passes is equal to 4 mm and the distance between the pellet and the Raman probe (approximately 1 mm) is adjustable, in order to optimize the signal intensity. The temperature on the pellet is controlled via a thermocouple placed on the sample holder. This temperature was thus used as a reference to command the heat controllers in order to avoid any perturbation of the heat transfer with the dedicated steel barrel holding the Raman probe compared to the original reactor with only KBr windows.

The cell is placed in a IR spectrometer bench (here is a Nicolet 6700 FT-IR spectrometer equipped with a MCT/A detector) allowing the recording of the transmission IR spectra (64 scans/spectrum, 2 cm^{-1} resolution). For Raman, the laser (532 nm) beam generated by a Horiba Jobin Yvon Labram300 spectrometer is guided into the cell by an optical fiber and focused on the sample with an *ad hoc InPhotonics* Raman probe specially designed to withstand high temperatures. Spectrum resolution was about 1.5 cm^{-1} and laser power was around 5 mW on the sample. It can be noted that at the end of the experiments, the pellet did not show any sign of local overheating or preferential carbon deposit in the analysis zone of the Raman laser. The dual IR-Raman *operando* reactor can be heated for catalyst activation or reaction, and can be fed with controlled gas flow. Downstream the catalyst wafer, the exhaust gases are directed towards an IR gas cell, a GC and/or a mass spectrometer for simultaneous on line analysis. The current approach has, thus, the advantage

of the simultaneous monitoring of Raman and transmission IR spectra while acquiring relevant catalytic data, and easy adaptability on any FTIR and fibre-coupled Raman spectrometers.

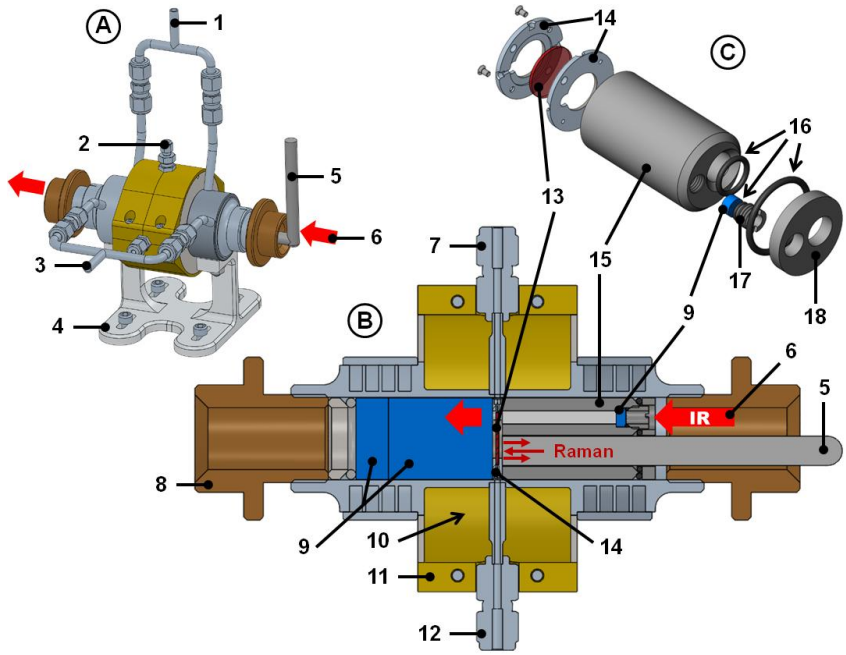

Figure 1. *Description of the IRRaman device adapted from the Sandwich cell: (A) general view of the cell in perspective, (B) longitudinal view and (C) exploded view of the IRRAMAN accessory. (1) air cooling outlet, (2) thermocouple location, (3) air cooling inlet, (4) IRRAMAN cell support, (5) Raman probe, (6) IR beam, (7) gas outlet, (8) adjusting nut for airtightness, (9) KBr windows, (10) oven location, (11) external shell, (12) gas inlet, (13) sample (wafer), (14) wafer holder, (15) barrel of the IRRAMAN accessory, (16) Kalrez O-ring, (17) hollow clamping nut (for the passage of the IR beam), (18) cap of the IRRAMAN accessory.*

ODH reaction conditions. Three catalytic materials (Zr-V2.5, Zr-V5.0 and Zr-V6.4) were tested in the propane oxidative dehydrogenation (ODH) in the IRRaman *operando* reactor. For all the experiments, the samples were pressed into self-supported wafers. The weight of catalyst (W_{cat}) and the total volumetric

gas flow (F_T) were around 31.5 mg and 18.1 mL·min^{-1}, respectively, resulting in a space-time (W_{cat}/F_{C3H8}) of 0.53 g_{cat}·s·mL$^{-1}{}_{C3H8}$. The reaction temperature was varied from 200 to 340ºC. Two different gas mixtures so called "activation" and "reaction" flows were used. The activation flow consisted of a mixture containing 10% of oxygen in argon, while the reaction flow consisted of a mixture of 20% of propane and 10% of oxygen in argon. Experiments without oxygen were also carried out for both the activation and the reaction flow (noted DH in this case). Gas lines were heated at 60ºC before and after the reaction-cell in order to pre-heat the reactant mixture and to avoid condensation of products leaving the reactor-cell.

The experiments were performed after the dehydration of the samples by a treatment under activation flow from room temperature to 340ºC with a heating rate of 5ºC·min^{-1}. After activation and equilibration at the reaction temperature, different flows were alternated in the following order: activation, reaction, activation, reaction without oxygen, and activation flow. Sometimes, the activation flow without oxygen was introduced between the reaction and the activation flow with oxygen, in order to observe the influence of oxygen in the changes of the catalyst. The conditions were never changed before achieving the steady state in each experiment.

Operando FTIR and *operando* Raman spectra of the catalysts were acquired every 2 and 4 min, respectively. Reactants and products of the gas phase were analyzed by both an online FTIR gas cell (one spectrum every 2 min), and online mass spectrometry (one measurement every ~3 seconds). In all the experiments performed under reaction flow the carbon molar balances were

attained with a maximum error of 5%. Propane conversion and the selectivity to product "i" are denoted as $X_{C_3H_8}$ and S_i, respectively, being:

$$X_{C_3H_8}(\%) = \frac{F_{0,C_3H_8} - F_{C_3H_8}}{F_{0,C_3H_8}} 100 \quad (1)$$

$$S_i(\%) = \frac{n_i F_i}{n_{C_3H_8} F_{0,C_3H_8} X_{C_3H_8}} 100 \quad (2)$$

where F_{0,C_3H_8} and $F_{C_3H_8}$ are the molar flows of propane in the inlet and in the outlet streams, respectively. F_i is the molar flow of i product in the outlet stream, and n_i is the number of carbon atoms per molecule of i product ($n_{C_3H_8} = 3$). Turn-over frequency (TOF) was calculated from Eq. (3); it quantifies the specific activity under defined reaction conditions per vanadium atom describing the number of converted moles of propane per mol of vanadium and time:

$$TOF = \frac{F_{0,C_3H_8} X_{C_3H_8} M_V}{W_{cat} W_V} \quad (3)$$

where M_V is denoted as the molar mass of vanadium and W_V mass of vanadium per gram catalyst based on nominal loading or determined by XPS in a previous work [48].

Blank experiments were performed under reaction flow without catalyst and with a vanadium-free zirconia sample, in order to discard a possible contribution of the homogeneous phase reaction and/or of the zirconia support in the catalytic results of propane ODH at the temperatures studied. In both cases propane conversion values were negligible.

Results and Discussion

1) Monitoring of the pre-activation of the catalysts

Before reaction, the catalysts can be followed during the initial activation step. Figure 2 shows the simultaneous Raman and infrared spectra of hydrated and dehydrated samples. This approach allows the determination of all the vibrational bands from 5000 cm^{-1} to 150 cm^{-1}, without the restrictions usually observed in IR spectroscopy of the solids, where lattice bands absorb all the signal below ca. 1000 cm^{-1}. All solids show broad Raman bands (642, 459, 314 and 268 cm^{-1}) associated with the tetragonal phase of zirconia [48,54], in agreement with the XRD results (Supporting Information, Figure S1); these bands are not sensitive to hydration/dehydration (Figure 2B) and are used to normalize the intensity of Raman spectra. The infrared bands near 1630 cm^{-1} and at 3500-3400 cm^{-1} show the presence of adsorbed water in all samples at room temperature (Figure 2A); these bands are respectively attributed to the H-O-H bending and v(OH) stretching modes [55-56]. The infrared signal of adsorbed water molecules increases with vanadia content and it is removed upon dehydration (Figure 2A). Weak bands due to the hydroxyls on the solid are then visible around 3700 cm^{-1}. The Raman and infrared V=O modes near 1020 cm^{-1} [57-58] red-shift upon hydration; these are characteristic of molecularly dispersed vanadium oxide species [59]. The infrared and Raman modes V=O in dehydrated samples blue-shift from 1019 to 1029 cm^{-1} as the vanadium content increases from 2.5 to 6.4% (w/w), due to a higher relative population of polyvanadates with respect to monovonadates [59]. It is important to underline the highly consistent wavenumbers observed for the V=O mode in both Raman and infrared systems with vanadia loading, for dehydrated samples, which match at the same values (Figure 3). This implies that the cell design and the

neighboring spots of analysis for IR and Raman are well-suited for the measurements in exactly the same conditions.

No additional information may be extracted from infrared spectra below 900 cm^{-1}, due to the strong absorption of zirconia support. Conversely, Raman spectroscopy does provide additional information of vanadia species in that spectral window: the broad Raman signal in the 700-950 cm^{-1} range grows stronger with vanadium content and corresponds to V-O-V and V-O-Zr modes [48,60], the signal for V-O-V chains appears near 880 cm^{-1} [61], while the broad signal near 770 cm^{-1} is assigned to V-O-Zr vibrations like in ZrV_2O_7 samples [48,62]. Since V_2O_5 presents intense Raman bands near 143 and 994 cm^{-1} [61], its presence can be excluded in these samples. Infrared spectra provide additional complementary information. The infrared bands near 1580, 1456 and a shoulder near 1380 cm^{-1} present in the dehydrated samples are attributed to carbonaceous deposits. In particular, the band at 1580 cm^{-1} is characteristic of C=C bond stretching in polycyclic aromatic compounds, while the weaker bands near 1456 and 1380 cm^{-1} have been attributed to the bending modes of –CH, -CH_2 and –CH_3 species in carbonaceous deposits [63-64]. The presence of bidentate carbonates (weak features at about 1550, 1315 and 1060 cm^{-1}) [65] cannot be excluded as well. The sharp band near 2339 cm^{-1} is associated with occluded CO_2 [66-67] that could be retained in the materials closed porosity. This CO_2 may form during the preparation of the samples in the calcination step of the carbonaceous precursors.

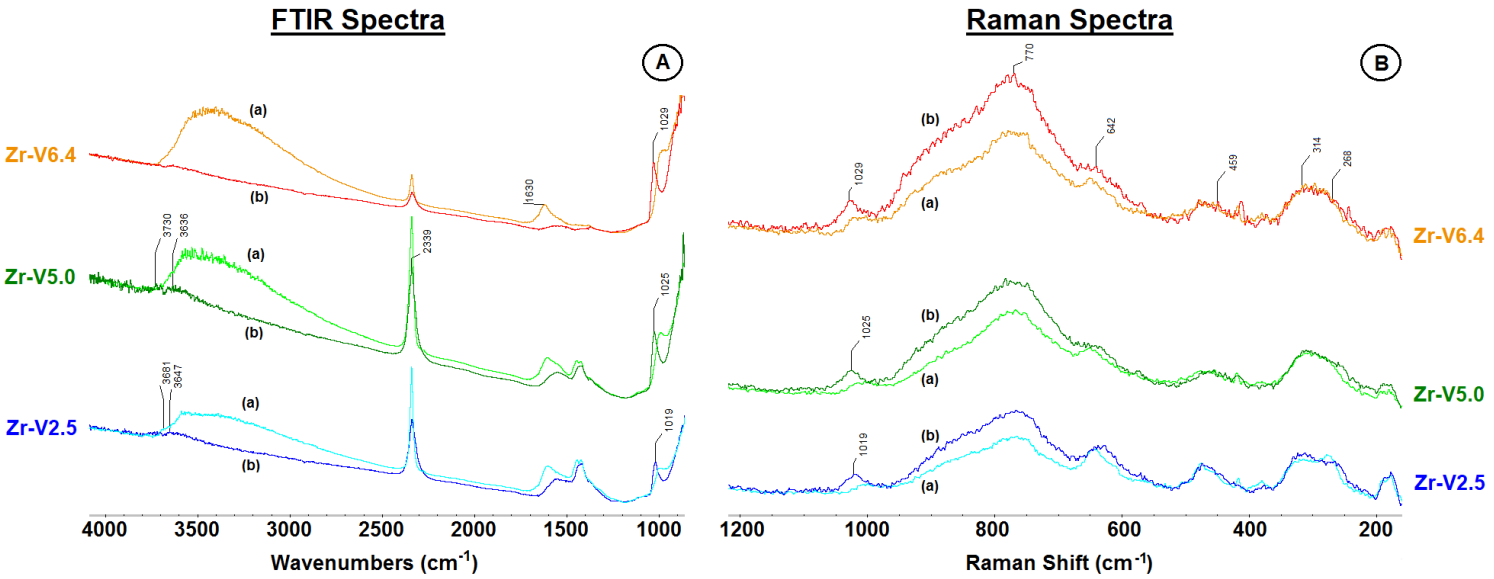

Figure 2. *FTIR (A-left) and Raman (B-right) spectra obtained in the reactor under activation flow (10% O_2 in Ar) at room temperature (a) and at 340ºC (b).*

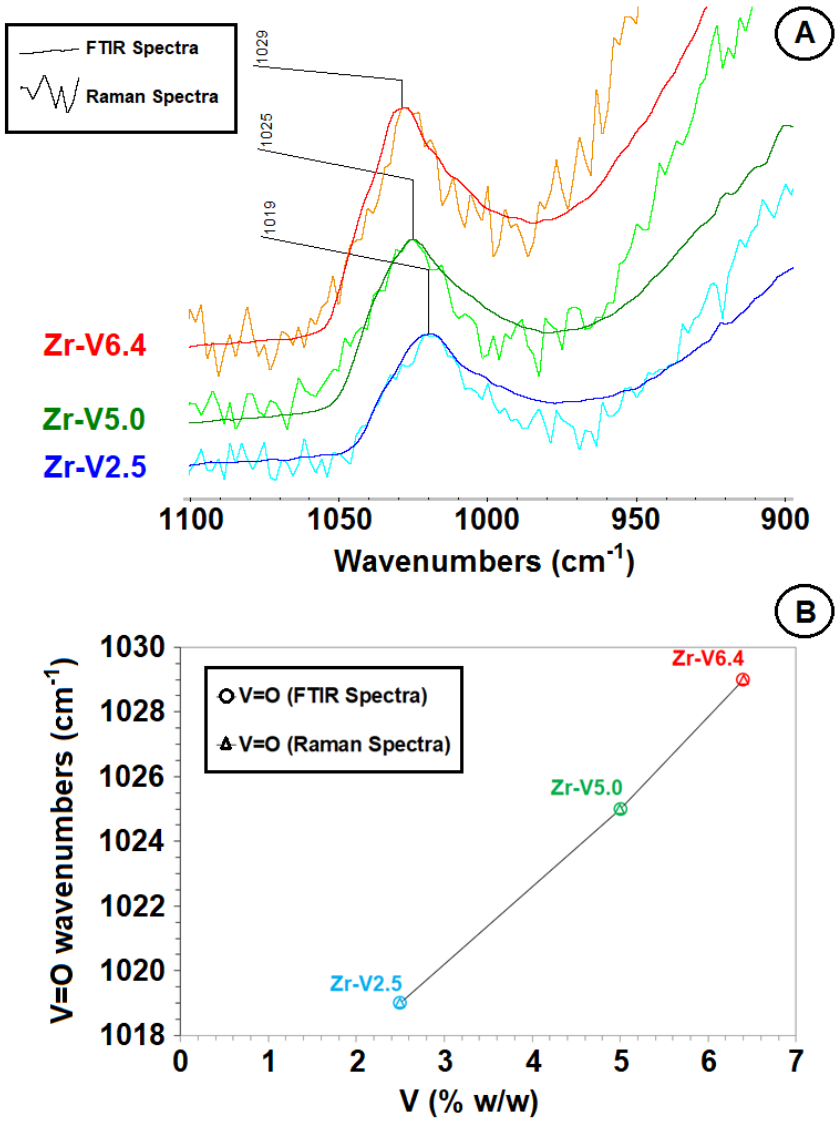

Figure 3. *A (top). Infrared and Raman spectra in the V=O region for dehydrated catalysts. B (bottom). (○) Infrared and (Δ) Raman V=O mode frequency vs. vanadia loading for dehydrated catalysts.*

2) Studying catalysts during reaction

The evaluation of the IRRaman reactor in reactive conditions is presented in this section. Table 1 shows the activity results obtained during propane ODH experiments in the IRRaman reactor at 340ºC and measured via the Mass Spectrometer signal and FTIR spectra from the gas phase. These results are consistent with those obtained with the same samples in a conventional fixed bed microreactor [48], which validates the IRRaman reactor as providing catalytically relevant data (i.e., as a genuine *operando* reactor) and adequate temperature control. The TOF values are calculated assuming that all vanadium atoms are exposed on the catalysts, which is not strictly the case. Nevertheless, the fact that TOF calculated from XPS or from the nominal values are similar, enables at least a qualitative use of the evolution of these calculated values. Catalysts were all inactive at 200°C. Conversions then gradually increased. Finally at 340°C their activity increases with the vanadium content for the studied conditions, as indicated by the conversion, yield to propylene and TOF.

Table 1. *Activity results obtained during the operando experiments in the IRRaman reactor at 340ºC (Catalyst weight: ~31.5 mg, Total Flow: ~18,1 mL·min^{-1}, Space-time: ~0.53 g·s·mLC_3^{-1}).*

Sample	X_{C3H8} (%)	X_{O2} (%)	S_{C3H6} (%)	Y_{C3H6} (%)	TOF[a] (10^{-3}·s^{-1})	TOF[b] (10^{-3}·s^{-1})
Zr-V2.5	1.3	6.6	71.4	0.93	2.02	2,18
Zr-V5.0	3.2	10.9	75.8	2.42	2.74	2,69
Zr-V6.4	5.3	24.3	58.5	3.10	3.71	3,48

[a] TOF based on XPS analyses. [b] TOF based on nominal loading.

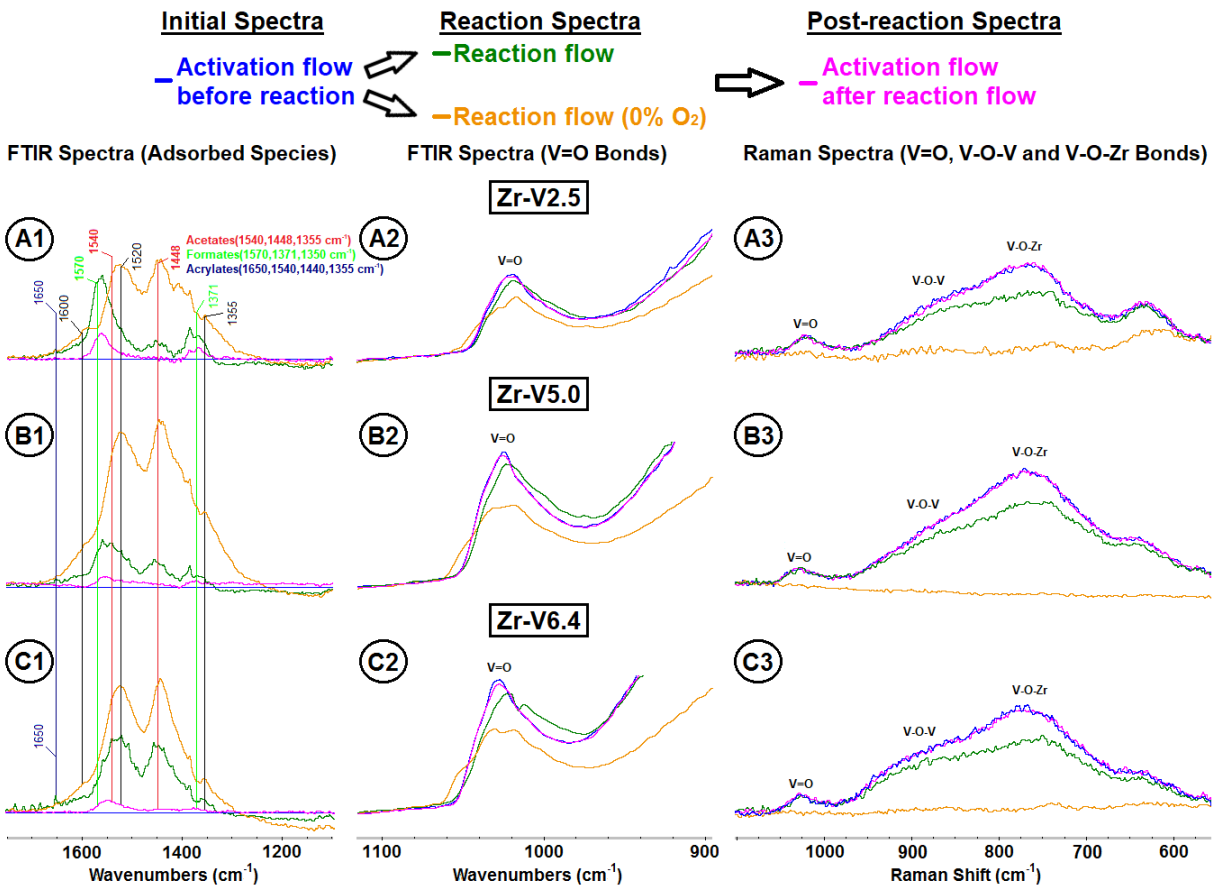

Figure 4. *Operando FTIR (1 and 2) and Raman spectra (3) for (A) Zr-V2.5, (B) Zr-V5.0 and (C) Zr-V6.4 at 340ºC. IR spectra shown at 1700-1100 cm^{-1} (1) were all subtracted with the reference spectrum of the sample under activation flow at the same temperature. Green and yellow traces represent experiments using ODH and DH feeds, respectively.* Spectra represented in green correspond directly to the activity results presented in Table 1. *Blue and pink traces represent experiments using activation flow before and after reaction, respectively.*

These activity data were compared with the evolution of the Raman and FTIR *operando* spectra (Figure 4). In order to fully characterize the catalysts, spectra were acquired at 340ºC both in the presence and absence of oxygen, and with an activation flow before and after reaction. FTIR spectra in the 1750-1100 cm^{-1} region provide information about the adsorbed oxygenated species (Figure 4-1). In the 1100-900 cm^{-1} region, FTIR bands related to V=O bonds are detected (Figure 4-2) and can be directly compared to the Raman results presented in the region 1100-525 cm^{-1} (Figure 4-3). Adsorbed species were removed by heat treatment in presence of O_2 before starting each experiment.

The catalysts exhibit some infrared bands in the region of adsorbed species during ODH reaction (green spectra in Figure 4-1). These bands correspond to a mixture of bidentate acetates (1540, 1448, and 1355 cm^{-1}), acrylates (~1640, 1540, 1440, and 1355 cm^{-1}) and bidentate formates (1570, 1371, and 1350 cm^{-1}) [70–75]. Interestingly, at 200°C, bands could also be observed in the same range but only for the highest vanadium loadings (Figure S2). In this case, formates were predominant and remained stable upon oxidation. All the catalysts being inactive at this temperature, formate species are thus likely to have a moderate role in the reaction scheme. Conversely, at 340°C, the adsorbed species are almost completely removed upon reoxidation (Figure 4, pink spectra); CO_x and water are detected in the gas phase, suggesting that these surface adsorbed species are intermediate of the total oxidation pathway. It can also be observed that the proportion of acetates and acrylates increases with respect to formates with the vanadium content of the catalysts, since the bands corresponding to acetate and acrylate species become more prominent, and especially in the most active catalyst (Zr-V6.4). This could also indicate that acetates and

acrylates preferentially adsorb on sites only present on the higher vanadium loadings, i.e. more polymerized species. A small shift and a slight intensity decrease of the infrared V=O modes (Figure 4-2) is apparent during reaction (green spectra) with respect to the initial spectra (blue profiles), this effect being more noticeable as vanadium content increases. These small perturbations observed during reaction (green spectra) disappear upon reoxidation (pink spectra) along with the concomitant removal of the above adsorbed oxygenate species. On the other hand, Raman spectra of all the catalysts (Figure 4-3) show a significant decrease in the intensity of the bands associated to V-O-V and V-O-Zr bonds in reaction conditions (green spectra) with respect to the initial spectra (blue profiles). These bands are restored under oxidizing conditions, since the post-reaction spectra (pink profiles) overlap with the initial spectra (blue profiles) in all cases.

In additional experiments, we introduced reaction feed without O_2 (DH; yellow spectra). These spectra show a higher amount of adsorbed oxygenates -especially acetates- than in ODH conditions (Figure 4-1). As reported in the literature [76], lattice oxygen is not involved in the formates conversion to CO. Conversely, the development of acetates and acrylates implies catalyst reduction (i.e., consumption of lattice oxygen). Therefore, during DH, acetates dominate because only the formates are removed. During ODH, both acetate and formate species are being formed and removed, giving rise to a steady state characterised by a spectrum which is just a mere linear combination of both IR spectra. These differences are not observed between the DH and ODH spectra for the catalysts with higher vanadium content (Zr-V5.0 and Zr-V6.4),

since they already present a high proportion of acetates with respect to formates.

During DH, carbonaceous deposits form, as evidenced by a shoulder around 1600 cm^{-1} in the FTIR spectra and Raman bands of carbon compounds around 1430 and 1600 cm^{-1} (Supporting Information, Figure S3). Moreover, there is a significant decrease of V=O, V-O-V and V-O-Zr modes intensity (Figure 4 A2-A3, B2-B3 and C2-C3, yellow spectra). While the V=O mode remains mildly affected, there is a large depletion of the polyvanadate Raman bands (Figure 4). The absence of changes after inert argon was fed after reaction demonstrates that the reoxidation of the catalyst (or the recovery of the vanadia bands to the initial state) and the removal of the adsorbed species (mainly acetates and carbonaceous deposits) are only possible if there is oxygen in the gas phase.

Comentado [HC1]: After reduction reaction we have observed that the V=O and polyvanadates have practically disappeared in Raman spectra, while in the case of IR the V=O mode are still remains. In our opinion this is due to the different way to obtained the measure, IR (transmission) and Raman (back-scatering)

Comentado [GC2]: The difference is strange indeed. I don't think it is related to the transmission/back-scattering because we would have differences all the time.
I rather wonder whether Raman is obscured in these reactive conditions, may be due to fluorescence in evolving conditions?

Comentado [M.D.3]: Your opinión Miguel and Olga?

V=O and V-O-V/V-O-Zr bands undergo changes during reaction, but the most important modifications are observed in the case of V-O-V and V-O-Zr bonds, suggesting that they participate to the reaction during propane ODH, being most probably the active sites. These changes are reversible and the bonds are restored under subsequent oxidation. These results are in agreement with previous findings that determine a higher reactivity of the bridging oxygen (V-O-V and V-O-Support) with respect to the terminal oxygen of the vanadyl group [77]. The perturbations observed in the V=O band could somehow be associated with the interaction of these bonds with the adsorbed species, since these shifts are only observed when these species are present, and they disappear just when the oxygenates are removed.

The evolution of reaction products during DH may also be monitored by the analysis of the gas phase by IR spectroscopy instead of Mass Spectrometry. The results for Zr-V6.4 at 340ºC are shown in Supporting Information, Figure S4. The initial products, as expected, are propylene, CO and CO_2, whose concentration decrease with time, as the lattice oxygen of the catalysts is being exhausted. The fact that these oxygenates products are being detected during some minutes, confirms the participation of lattice oxygen, in line with a Mars-Van Krevelen type mechanism. This is confirmed by the major decrease of the V-O-V/V-O-Zr bands, which suggests the contribution of these oxygen atoms to the oxidation. When oxygen is fed again, the activity, and the V-O-V/V-O-Zr bands, are recovered, demonstrating the reversibility of the redox behavior of these catalysts.

Therefore, while *operando* analysis is required to provide the necessary catalytic data, the simultaneous acquisition of IR and Raman spectra allows an extensive evaluation of both the adsorbed species and their impact on the working catalyst.

Conclusions

A new multimodal *operando* cell was developed for simultaneous Raman and FTIR *operando* spectrocopies ("IRRaman" reactor). This system is demonstrated here through the behavior of V-Zr-O catalysts under propane ODH conditions. The combination of complementary spectroscopies allows both the identification of the reaction intermediates (oxygenates species detected by FTIR) and additional structural information of the evolution of V=O and V-O-

V/V-O-Zr bonds on the catalysts (FTIR and Raman spectroscopy).The V=O mode has the same frequency in Raman and infrared since they are measured under identical conditions. The results are consistent with the reported Mars-van Krevelen mechanism. They also indicate that the V-O-V/V-O-Zr sites are more active than terminal V=O bonds, so shedding additional light on this industrially important reaction mechanism.

In perspective, the new *operando* device can provide fundamental insights into many reaction mechanisms, thanks to its capacity to associate concomitant information from the surface adsorbed species and catalyst structure evolution under stream in a single rig, on the same sample, at the same time and at identical operating conditions. This device could also find useful applications in the study of materials in evolution under heat and/or under controlled atmosphere.

Supporting information

XRD of the solids; Raman and FTIR spectra in ODH conditions at 200°C, Raman spectra of the solids during DH reaction (20% propane in He) at 300 and 340ºC; FTIR spectra of the gas phase for Zr-V6.4 during DH reaction (20% C_3H_8 in Ar) at 340ºC.

Acknowledgements

Authors acknowledge the FEDER-Region Basse-Normandie (France)-CNRS for a Chaire d'Excellence, which resulted in the implementation of the "IRRaman"

rig and a research stay allowing to perform these investigations. This work was also supported by the Spanish Ministry of Economy and Competitiveness and FEDER (CTQ2012-36408, CTQ2015-68654-R and CTM2017-82335-R). J.J.T.H. acknowledges the assistance of the Ministry of Economy and Competitiveness of Spain for the award of a FPI Grant (BES-2013-064425) and the award for performing his stay at ENSICAEN (EEBB-I-16-10749).

References

(1) Chakrabarti, A.; Ford, M. E.; Gregory, D.; Hu, R.; Keturakis, C. J.; Lwin, S.; Tang, Y.; Yang, Z.; Zhu, M.; Bañares, M. A.; et al. A Decade+ of Operando Spectroscopy Studies. *Catal. Today* **283**, 27–53 (2017), https://doi.org/10.1016/j.cattod.2016.12.012.

(2) Vimont, A.; Thibault-Starzyk, F.; Daturi, M. Analysing and Understanding the Active Site by IR Spectroscopy. *Chem. Soc. Rev*. **39** (12), 4928–4950 (2010). https://doi.org/10.1039/B919543M.

(3) Marie, O.; Bazin, P.; Daturi, M. Vibrational Spectroscopic Studies of Catalytic Processes on Oxide Surfaces. In Spectroscopic Properties of Inorganic and Organometallic Compounds; 2011; pp 34–103. https://doi.org/10.1039/9781849732833-00034.

(4) Meunier, F. C. The Design and Testing of Kinetically-Appropriate Operando Spectroscopic Cells for Investigating Heterogeneous Catalytic Reactions. *Chem. Soc. Rev.***39** (12), 4602–4614 (2010). https://doi.org/10.1039/B919705M.

(5) Frenkel, A. I.; Rodriguez, J. A.; Chen, J. G. Synchrotron Techniques for In Situ Catalytic Studies: Capabilities, Challenges, and Opportunities. *ACS Catal.*, **2 (11),** 2269–2280 *(*2012). https://doi.org/10.1021/cs3004006.

(6) Guerrero-Pérez, M. O.; Bañares, M. A. From Conventional in Situ to Operando Studies in Raman Spectroscopy. *Catal. Today* **113** (1), 48–57 (2006). https://doi.org/10.1016/j.cattod.2005.11.009.

(7) Bañares, M. A. Operando Methodology: Combination of in Situ Spectroscopy and Simultaneous Activity Measurements under Catalytic Reaction Conditions. *Catal. Today* **100** (1), 71–77 (2005). https://doi.org/10.1016/j.cattod.2004.12.017.

(8) Wachs, I. E.; Roberts, C. A. Monitoring Surface Metal Oxide Catalytic Active Sites with Raman Spectroscopy. *Chem. Soc. Rev.***39** (12), 5002–5017 (2010). https://doi.org/10.1039/C0CS00145G.

(9) Hunger, M.; Weitkamp, J. In Situ IR, NMR, EPR, and UV/Vis Spectroscopy: Tools for New Insight into the Mechanisms of Heterogeneous Catalysis. *Angew. Chem. - Int. Ed.* **40** (16), 2954–2971 (2001). https://doi.org/10.1002/1521-3773(20010817)40:16<2954::AID-ANIE2954>3.0.CO;2-#.

(10) Lysova, A. A.; Koptyug, I. V. Magnetic Resonance Imaging Methods for in Situ Studies in Heterogeneous Catalysis. *Chem. Soc. Rev.***39** (12), 4585–4601 (2010). https://doi.org/10.1039/B919540H.

(11) Schoonheydt, R. A. UV-VIS-NIR Spectroscopy and Microscopy of Heterogeneous Catalysts. *Chem. Soc. Rev.* **39** (12), 5051–5066 (2010). https://doi.org/10.1039/C0CS00080A.

(12) Tao, F.; Crozier, P. A. Atomic-Scale Observations of Catalyst Structures under Reaction Conditions and during Catalysis. *Chem. Rev.***116 (6)**, 3487–3539 (2016). https://doi.org/10.1021/cr5002657.

(13) Rousseau, S.; Marie, O.; Bazin, P.; Daturi, M.; Verdier, S.; Harlé, V. Investigation of Methanol Oxidation over Au/Catalysts Using Operando IR Spectroscopy: Determination of the Active Sites, Intermediate/Spectator Species, and Reaction Mechanism. *J. Am. Chem. Soc.***132** (31), 10832–10841 (2010). https://doi.org/10.1021/ja1028809.

(14) Rasmussen, S. B.; Bañares, M. A.; Bazin, P.; Due-Hansen, J.; Ávila, P.; Daturi, M. Monitoring Catalysts at Work in Their Final Form: Spectroscopic Investigations on a Monolithic Catalyst. *Phys. Chem. Chem. Phys.***14** (7), 2171–2177 (2012). https://doi.org/10.1039/C1CP22629K.

(15) Mul, G.; Hamminga, G. M.; Moulijn, J. A. Operando ATR-FTIR Analysis of Liquid-Phase Catalytic Reactions: Can Heterogeneous Catalysts Be Observed? *Vib. Spectrosc.* **34** (1), 109–121 (2004). https://doi.org/10.1016/j.vibspec.2003.07.004.

(16) Davó-Quiñonero, A.; Bueno-López, A.; Lozano-Castelló, D.; McCue, A. J.; Anderson, J. A. Rapid-Scan Operando InfraredSpectroscopy. *ChemCatChem* 8 (11), 1905–1908 (2016). https://doi.org/10.1002/cctc.201600302.

(17) J. Saussey; F. Thibault-Starzyk; B.M. Weckhuysen. In Situ Characterization of Catalysts; American Scientific Publishers: San Diego, 2004; pp 15–31.

(18) Brückner, A.; Kubias, B.; Lücke, B. In Situ-Electron Spin Resonance: A Useful Tool for the Investigation of Vanadium Phosphate Catalysts (VPO) under Working Conditions. *Catal. Today* **32** (1), 215–222 (1996). https://doi.org/10.1016/S0920-5861(96)00077-6.

(19) Bentrup, U.; Brückner, A.; Rüdinger, C.; Eberle, H.-J. Elucidating Structure and Function of Active Sites in VO_x/TiO_2 Catalysts during Oxyhydrative Scission of 1-Butene by in Situ and Operando Spectroscopy. *Appl. Catal. Gen.***269** (1), 237–248 (2004). https://doi.org/10.1016/j.apcata.2004.04.027.

(20) Clausen, B. S.; Steffensen, G.; Fabius, B.; Villadsen, J.; Feidenhans'l, R.; Topsøe, H. In Situ Cell for Combined XRD and On-Line Catalysis Tests: Studies of Cu-Based Water Gas Shift and Methanol Catalysts. *J. Catal*. **132** (2), 524–535 (1991). https://doi.org/10.1016/0021-9517(91)90168-4.

(21) Guerrero-Pérez, M. O.; López-Medina, R.; Rojas-Garcia, E.; Bañares, M. A. XANES Study of the Dynamic States of V-Based Oxide Catalysts under

Partial Oxidation Reaction Conditions. *Catal. Today* 336 (2019) 210-215 https://doi.org/10.1016/j.cattod.2017.12.016.

(22) Woo, S. I.; Hill Jr., C. G. In Situ Raman Spectroscopy Studies of the Hydroformylation of Propylene. *J. Mol. Catal.* **29** (2), 231–258 *(*1985). https://doi.org/10.1016/0304-5102(85)87007-3.

(23) Snyder, T. P.; Hill, C. G. Stability of Bismuth Molybdate Catalysts at Elevated Temperatures in Air and under Reaction Conditions. *J. Catal*. **132** (2), 536–555 (1991). https://doi.org/10.1016/0021-9517(91)90169-5.

(24) Wang, C.-B.; Deo, G.; Wachs, I. E. Interaction of Polycrystalline Silver with Oxygen, Water, Carbon Dioxide, Ethylene, and Methanol: In Situ Raman and Catalytic Studies. *J. Phys. Chem. B* **103** (27), 5645–5656 (1999).

(25) Tolia, A. A.; Williams, C. T.; Takoudis, C. G.; Weaver, M. J. Surface-Enhanced Raman Spectroscopy as an in-Situ Real-Time Probe of Catalytic Mechanisms at High Gas Pressures: The CO-NO Reaction on Rhodium. *J. Phys. Chem*. **99** (13), 4599–4608 (1995). https://doi.org/10.1021/j100013a034.

(26) Guerrero-Pérez, M. O.; Bañares, M. A. Operando Raman Study of Alumina-Supported Sb–V–O Catalyst during Propane Ammoxidation to Acrylonitrile with on-Line Activity Measurement. *Chem. Commun.***12**, 1292–1293 (2002). https://doi.org/10.1039/B202556F.

(27) Guerrero-Pérez, M. O.; Bañares, M. A. Operando Raman−GC Study of Supported Alumina Sb- and V-Based Catalysts: Effect of Sb/V Molar Ratio and Total Sb+V Coverage in the Structure of Catalysts during Propane

Ammoxidation. *J. Phys. Chem. C* **111**(3), 1315–1322 *(*2007). https://doi.org/10.1021/jp065387s.

(28) Guerrero-Pérez, M. O.; Rojas, E.; Gutiérrez-Alejandre, A.; Ramírez, J.; Sánchez-Minero, F.; Fernández-Vargas, C.; Bañares, M. A. In Situ Raman Studies during Sulfidation, and Operando Raman-GC during Ammoxidation Reaction Using Nickel-Containing Catalysts: A Valuable Tool to Identify the Transformations of Catalytic Species. *Phys. Chem. Chem. Phys.* **13** (20), 9260–9267 *(*2011). https://doi.org/10.1039/C0CP02242J.

(29) López-Medina, R.; Fierro, J. L. G.; Guerrero-Pérez, M. O.; Bañares, M. A. Structural Changes Occurring at the Surface of Alumina-Supported Nanoscaled Mo–V–Nb–(Te)–O Catalytic System during the Selective Oxidation of Propane to Acrylic Acid. *Appl. Catal. Gen.* **406** (1), 34–42 (2011). https://doi.org/10.1016/j.apcata.2011.08.002.

(30) Weckhuysen, B. M. Determining the Active Site in a Catalytic Process: Operando Spectroscopy Is More than a Buzzword. *Phys. Chem. Chem. Phys.* **5** (20), 4351–4360 (2003). https://doi.org/10.1039/B309650P.

(31) Mondelli, C.; Ferri, D.; Grunwaldt, J.-D.; Krumeich, F.; Mangold, S.; Psaro, R.; Baiker, A. Combined Liquid-Phase ATR-IR and XAS Study of the Bi-Promotion in the Aerobic Oxidation of Benzyl Alcohol over Pd/Al_2O_3. *J. Catal.***252** (1), 77–87 (2007). https://doi.org/10.1016/j.jcat.2007.09.013.

(32) Cats, K. H.; Weckhuysen, B. M. Combined Operando X-Ray Diffraction/Raman Spectroscopy of Catalytic Solids in the Laboratory: The

Co/TiO_2 Fischer–Tropsch Synthesis Catalyst Showcase. *ChemCatChem* **8**(8), 1531–1542 (2016). https://doi.org/10.1002/cctc.201600074.

(33) Beale, A. M.; Eerden, A. M. J. van der; Kervinen, K.; Newton, M. A.; Weckhuysen, B. M. Adding a Third Dimension to Operando Spectroscopy: A Combined UV-Vis, Raman and XAFS Setup to Study Heterogeneous Catalysts under Working Conditions. *Chem. Commun*. **24**, 3015–3017 (2005). https://doi.org/10.1039/B504027B.

(34) Patlolla, A.; Carino, E. V.; Ehrlich, S. N.; Stavitski, E.; Frenkel, A. I. Application of Operando XAS, XRD, and Raman Spectroscopy for Phase Speciation in Water Gas Shift Reaction Catalysts. *ACS Catal*. **2** (11), 2216–2223 (2012). https://doi.org/10.1021/cs300414c.

(35) Brückner, A. Killing Three Birds with One Stone—Simultaneous Operando EPR/UV-Vis/Raman Spectroscopy for Monitoring Catalytic Reactions. Chem. Commun. 2005, No. 13, 1761–1763. https://doi.org/10.1039/B418790C.

(36) Bentrup, U. Combining in Situ Characterization Methods in One Set-up: Looking with More Eyes into the Intricate Chemistry of the Synthesis and Working of Heterogeneous Catalysts. *Chem. Soc. Rev.* **39** (12), 4718–4730 (2010). https://doi.org/10.1039/B919711G.

(37) Airaksinen, S. M. K.; Krause, A. O. I.; Sainio, J.; Lahtinen, J.; Chao, K.; Guerrero-Pérez, M. O.; Bañares, M. A. Reduction of Chromia/Alumina Catalyst Monitored by DRIFTS-Mass Spectrometry and TPR-Raman Spectroscopy.

Phys. Chem. Chem. Phys. **5** (20), 4371–4377 (2003). https://doi.org/10.1039/B305802F.

(38) Bourdon, G. L.; Adar, F.; Moreau, M.; Morel, S.; Reffner, J.; Mamede, A.-S.; Dujardin, C.; Payen, E. In Situ Characterization by Raman and IR Vibrational Spectroscopies on a Single Instrument: DeNOx Reaction over a Pd/γ-Al2O3 Catalyst. *Phys. Chem. Chem. Phys.* **5** (20), 4441–4444 (2003). https://doi.org/10.1039/B306045B.

(39) Li, G.; Hu, D.; Xia, G.; White, J. M.; Zhang, C. High Throughput Operando Studies Using Fourier Transform Infrared Imaging and Raman Spectroscopy. *Rev. Sci. Instrum*. **79** (7), 074101 (2008). https://doi.org/10.1063/1.2949389.

(40) Li, G.; Hu, D.; Xia, G.; Conrad, Zhang, Z. Methanol Partial Oxidation on MoO_3/SiO_2 Catalysts: Application of Vibrational Spectroscopic Imaging Techniques in a High Throughput Operando Reactor. *Top. Catal.* **52** (10), 1381–1387 (2009). https://doi.org/10.1007/s11244-009-9325-y.

(41) Urakawa, A.; Maeda, N.; Baiker, A. Space- and Time-Resolved Combined DRIFT and Raman Spectroscopy: Monitoring Dynamic Surface and Bulk Processes during NO_x Storage Reduction. *Angew. Chem. Int. Ed.* **4**7 (48), 9256–9259 (2008). https://doi.org/10.1002/anie.200804077.

(42) Visconti, C. G.; Lietti, L.; Manenti, F.; Daturi, M.; Corbetta, M.; Pierucci, S.; Forzatti, P. Spectrokinetic Analysis of the NOx Storage Over a Pt–Ba/Al_2O_3 Lean NO_x Trap Catalyst. *Top. Catal.* **56** (1), 311–316 (2013). https://doi.org/10.1007/s11244-013-9972-x.

(43) Grabowski, R. Kinetics of Oxidative Dehydrogenation of C2-C3 Alkanes on Oxide Catalysts. C*atal. Rev. - Sci. Eng.* **48** (2), 199–268 (2006). https://doi.org/10.1080/01614940600631413.

(44) Carrero, C. A.; Schloegl, R.; Wachs, I. E.; Schomaecker, R. Critical Literature Review of the Kinetics for the Oxidative Dehydrogenation of Propane over Well-Defined Supported Vanadium Oxide Catalysts. *ACS Catal.*, 4 (10), 3357–3380 (2014). https://doi.org/10.1021/cs5003417.

(45) Cavani, F.; Ballarini, N.; Cericola, A. Oxidative Dehydrogenation of Ethane and Propane: How Far from Commercial Implementation? *Catal. Today* **127** (1–4), 113–131 (2007). https://doi.org/10.1016/j.cattod.2007.05.009.

(46) Kung, H. H. Oxidative Dehydrogenation of Light (C2 to C4) Alkanes. In Advances in Catalysis; Eley, D. D., Pines, H., Haag, W. O., Eds.; Academic Press, 1994; Vol. 40, pp 1–38. https://doi.org/10.1016/S0360-0564(08)60655-0.

(47) Chakraborty, S.; Nayak, S. C.; Deo, G. TiO2/SiO2 Supported Vanadia Catalysts for the ODH of Propane. *Catal. Today* **254**, 62–71 (2015). https://doi.org/10.1016/j.cattod.2015.01.047.

(48) Ternero-Hidalgo, J. J.; Torres-Liñán, J.; Guerrero-Pérez, M. O.; Rodríguez-Mirasol, J.; Cordero, T. Electrospun Vanadium Oxide Based Submicron Diameter Fiber Catalysts. Part I: Preparation Procedure and Propane ODH Application. *Catal. Today* **325,** 131-143 (2019). https://doi.org/10.1016/j.cattod.2018.10.073.

(49) Ternero-Hidalgo, J. J.; Guerrero-Pérez, M. O.; Rodríguez-Mirasol, J.; Cordero, T. Electrospun Vanadium Oxide Based Submicron Diameter Fiber

Catalysts. Part II: Effect of Chemical Formulation and Dopants. *Catal. Today* 325, 144-150 (2019). https://doi.org/10.1016/j.cattod.2018.10.072.

(50) Wuttke, S.; Bazin, P.; Vimont, A.; Serre, C.; Seo, Y.-K.; Hwang, Y. K.; Chang, J.-S.; Férey, G.; Daturi, M. Discovering the Active Sites for C3 Separation in MIL-100(Fe) by Using Operando IR Spectroscopy. *Chem. – Eur. J.* **18** (38), 11959–11967 (2012). https://doi.org/10.1002/chem.201201006.

(51) Thomas, S.; Marie, O.; Bazin, P.; Lietti, L.; Visconti, C. G.; Corbetta, M.; Manenti, F.; Daturi, M. Modelling a Reactor Cell for Operando IR Studies: From Qualitative to Fully Quantitative Kinetic Investigations. *Catal. Today* **283**, 176–184 (2017). https://doi.org/10.1016/j.cattod.2016.07.008.

(52) Rasmussen, S. B.; Perez-Ferreras, S.; Bañares, M. A.; Bazin, P.; Daturi, M. Does Pelletizing Catalysts Influence the Efficiency Number of Activity Measurements? Spectrochemical Engineering Considerations for an Accurate Operando Study. *ACS Catal.* **3** (1), 86–94 (2013). https://doi.org/10.1021/cs300687v.

(53) El-Roz, M.; Bazin, P.; Thibault-Starzyk, F. An Operando-IR Study of Photocatalytic Reaction of Methanol on New *BEA Supported TiO_2 Catalyst. *Catal. Today* **205**, 111–119 (2013). https://doi.org/10.1016/j.cattod.2012.08.023.

(54) Fernandez, L.; Sanchez, E.; Panizza, M.; Carnasciali, M. M.; Busca, G. Vibrational and Electronic Spectroscopic Properties of Zirconia Powders. *J. Mater. Chem.* **11** (7), 1891–1897 (2001). https://doi.org/10.1039/b100909p.

(55) Ward, J. W. Nature of Sites Formed on Zeolites by Addition of Water. *J. Phys. Chem.* **72** (7), 2689–2690 (1968). https://doi.org/10.1021/j100853a090.

(56) Ward, J. W. The Nature of Active Sites on Zeolites: IV. The Influence of Water on the Acidity of X and Y Type Zeolites. *J. Catal.* **11** (3), 238–250 *(*1968). https://doi.org/10.1016/0021-9517(68)90037-7.

(57) Lietti, L.; Forzatti, P.; Ramis, G.; Busca, G.; Bregani, F. Potassium Doping of Vanadia/Titania de-NOxing Catalysts: Surface Characterisation and Reactivity Study. *Appl. Catal. B Environ.* **3** (1), 13–35 (1993). https://doi.org/10.1016/0926-3373(93)80065-L.

(58) Magg, N.; Immaraporn, B.; Giorgi, J. B.; Schroeder, T.; Bäumer, M.; Döbler, J.; Wu, Z.; Kondratenko, E.; Cherian, M.; Baerns, M.; et al. Vibrational Spectra of Alumina- and Silica-Supported Vanadia Revisited: An Experimental and Theoretical Model Catalyst Study. *J. Catal.***226** (1), 88–100 (2004). https://doi.org/10.1016/j.jcat.2004.04.021.

(59) Wachs, I. E. Raman and IR Studies of Surface Metal Oxide Species on Oxide Supports: Supported Metal Oxide Catalysts. *Catal. Today* **27** (3), 437–455 (1996). https://doi.org/10.1016/0920-5861(95)00203-0.

(60) Bañares, M. A.; Wachs, I. E. Molecular Structures of Supported Metal Oxide Catalysts under Different Environments. *J. Raman Spectrosc.* **33** (5), 359–380 *(*2002). https://doi.org/10.1002/jrs.866.

(61) Guerrero-Pérez, M. O.; Fierro, J. L. G.; Vicente, M. A.; Bañares, M. A. Effect of Sb/V Ratio and of Sb + V Coverage on the Molecular Structure and Activity of Alumina-Supported Sb-V-O Catalysts for the Ammoxidation of Propane to Acrylonitrile. *J. Catal.* **206** (2), 339–348 *(*2002). https://doi.org/10.1006/jcat.2001.3494.

(62) Christodoulakis, A.; Machli, M.; Lemonidou, A. A.; Boghosian, S. Molecular Structure and Reactivity of Vanadia-Based Catalysts for Propane Oxidative Dehydrogenation Studied by in Situ Raman Spectroscopy and Catalytic Activity Measurements. *J. Catal.* **222** (2), 293–306 *(*2004). https://doi.org/10.1016/j.jcat.2003.10.007.

(63) Eisenbach, D.; Gallei, E. Infrared Spectroscopic Investigations Relating to Coke Formation on Zeolites: I. Adsorption of Hexene-1 and n-Hexane on Zeolites of Type Y. *J. Catal.* **56** (3), 377–389 (1979). https://doi.org/10.1016/0021-9517(79)90130-1.

(64) Datka, J.; Sarbak, Z.; Eischens, R. P. Infrared Study of Coke on Alumina and Zeolite. *J. Catal*. **145** (2), 544–550 (1994). https://doi.org/10.1006/jcat.1994.1065.

(65) Daturi, M.; Binet, C.; Lavalley, J. C.; Blanchard, G. Surface FTIR Investigations on $Ce_xZr_{1-x}O_2$ System. *Surf. Interface Anal.* 3**0** (1), 273–277 (2000). https://doi.org/10.1002/1096-9918(200008)30:1<273::AID-SIA715>3.0.CO;2-G.

(66) Bando, K. K.; Sayama, K.; Kusama, H.; Okabe, K.; Arakawa, H. In-Situ FT-IR Study on CO_2 Hydrogenation over Cu Catalysts Supported on SiO_2, Al_2O_3, and TiO_2. *Appl. Catal. Gen.* **165** (1), 391–409 (1997). https://doi.org/10.1016/S0926-860X(97)00221-4.

(67) Ramis, G.; Busca, G.; Lorenzelli, V. Low-Temperature CO2 Adsorption on Metal Oxides: Spectroscopic Characterization of Some Weakly Adsorbed

Species. *Mater. Chem. Phys.***29** (1), 425–435 (1991). https://doi.org/10.1016/0254-0584(91)90037-U.

(68) Dinse, A.; Frank, B.; Hess, C.; Habel, D.; Schomäcker, R. Oxidative Dehydrogenation of Propane over Low-Loaded Vanadia Catalysts: Impact of the Support Material on Kinetics and Selectivity. *J. Mol. Catal. Chem.* **289** (1–2), 28–37 (2008). https://doi.org/10.1016/j.molcata.2008.04.007.

(69) Blasco, T.; Nieto, J. M. L. Oxidative Dyhydrogenation of Short Chain Alkanes on Supported Vanadium Oxide Catalysts. *Appl. Catal. Gen.* **157** (1), 117–142 (1997). https://doi.org/10.1016/S0926-860X(97)00029-X.

(70) Sanchez Escribano, V.; Busca, G.; Lorenzelli, V. Fourier Transform Infrared Spectroscopic Studies of the Reactivity of Vanadia-Titania Catalysts toward Olefins. 1. Propylene. *J. Phys. Chem.* **94** (26), 8939–8945 (1990). https://doi.org/10.1021/j100389a017.

(71) Baldi, M.; Finocchio, E.; Pistarino, C.; Busca, G. Evaluation of the Mechanism of the Oxy-Dehydrogenation of Propane over Manganese Oxide. *Appl. Catal. Gen.* **173** (1), 61–74 (1998). https://doi.org/10.1016/S0926-860X(98)00129-X.

(72) El-Roz, M.; Bazin, P.; Daturi, M.; Thibault-Starzyk, F. Operando Infrared (IR) Coupled to Steady-State Isotopic Transient Kinetic Analysis (SSITKA) for Photocatalysis: Reactivity and Mechanistic Studies. *ACS Catal.* **3** (12), 2790–2798 (2013). https://doi.org/10.1021/cs4006088.

(73) Alcock, N. W.; Tracy, V. M.; Waddington, T. C. Acetates and Acetato-Complexes. Part 2. Spectroscopic Studies. *J. Chem. Soc. Dalton Trans*. **21**, 2243–2246 (1976). https://doi.org/10.1039/DT9760002243.

(74) Collins, S. E.; Baltanás, M. A.; Bonivardi, A. L. An Infrared Study of the Intermediates of Methanol Synthesis from Carbon Dioxide over Pd/β-Ga_2O_3. *J. Catal*. **226** (2), 410–421 (2004). https://doi.org/10.1016/j.jcat.2004.06.012.

(75) Davydov, A. Molecular spectroscopy of oxide catalyst surfaces, Wiley, 2003, p. 454.

(76) Finocchio, E.; Busca, G.; Lorenzelli, V.; Escribano, V. S. FTIR Studies on the Selective Oxidation and Combustion of Light Hydrocarbons at Metal Oxide Surfaces. Part 2.—Propane and Propene Oxidation on Co_3O_4. *J. Chem. Soc. Faraday Trans.* 92 (9), 1587–1593 (1996). https://doi.org/10.1039/FT9969201587.

(77) Lewandowska, A. E.; Calatayud, M.; Lozano-Diz, E.; Minot, C.; Bañares, M. A. Combining Theoretical Description with Experimental in Situ Studies on the Effect of Alkali Additives on the Structure and Reactivity of Vanadium Oxide Supported Catalysts. *Catal. Today* **139** (3), 209–213 (2008). https://doi.org/10.1016/j.cattod.2008.04.049.